23rd ABCM International Congress of Mechanical Engineering
December 6-11, 2015, Rio de Janeiro, RJ, Brazil

NUMERICAL STUDY OF A BUBBLING FLUIDIZED BED USING A COMBINED CFD-DEM CODE

Marcelo José Alba
Universidade Tecnológica Federal do Paraná / Universidade Estadual de Maringá
marceloalba@utfpr.edu.br

Flávio Clareth Colman
Universidade Estadual de Maringá
fccolman@uem.br

Luiz Mário de Matos Jorge
Universidade Estadual de Maringá
lmmj@deq.uem.br

Alexandre Marconi de Souza da Costa
Universidade Estadual de Maringá
amscosta@uem.br

Paulo Roberto Paraíso
Universidade Estadual de Maringá
paulo@deq.uem.br

Abstract. *Fluidized beds are used in industries in the separation, mixing, drying and combustion operations. This work analyzed the behavior of a fluidized bed with the open-source MFIX-DEM code developed by the National Energy Technology Laboratory (NETL-USA). For the code, the gas and solid phases are treated in an Eulerian-Lagrangian framework. For the gas-phase, continuity and momentum conservation equations were solved. For the particles, or the solid-phase, was used the Discrete Element Method (DEM), which describes the contact and collisions phenomenon's from the spring-dashpot-friction concepts, by means of an explicit numerical approach. A two-dimensional grid with gas injection was used through a distributor at the bottom of the bed. The granular material analyzed was the soybeans. The gas velocity was varied to determine the influence of pressure drop within the bed. The results obtained by the different drag relationships were compared with the fluidization curves from the experimental data. A good approximation was observed mainly in the prediction of fluidizing behavior and stipulation of the minimum fluidization velocity. Significant differences were observed when comparing the experimental and numerical values of the pressure drop.*

Keywords: *fluidized bed, soybean, MFIX-DEM*

1. INTRODUCTION

Fluidized bed systems are extensively employed in several industries such as: agroindustry, chemical and pharmaceutical (Kunii and Levenspiel, 1991). Generally, fluidized systems allow significant improvements in heat and mass exchanges, with associated space and monetary revenues. Nowadays, a great portion gas-solids system studies takes advantage of easily available computational resources to predict the heat and mass transfer behavior of fluidized beds.

For the case of soybean grains, fluidized and spouted beds equipment are used to transfer heat through hot air injection. The heat transfer is accompanied by a noticeable moisture reduction. This process is important for a prolonged storage of the product, avoiding microorganism wastage (Soponronnarit, *et al*., 2001).

Spouted beds are the preferred fluidization routine for soybean grains, as the grains are classified in the Geldart D group. In addition, fluidized bed drying is recognized as a fast drying technology, due to the large air to product contact area achieved relative to a static bed caused by fluidization of the product, and the high air speed and high temperatures used (Soponronnarit *et al*., 2001). Soybean grains are particularly feasible for studies using the Discrete Element Method (DEM) (Tsuji, *et al*., 1993). This feasibility resides in the circularity and sphericity properties, with great uniformity in the particle diameter.

The CFD (Computational Fluid Dynamics) methodology when applied to research, development and optimization in the process industries can lead to relevant cost reduction. This economies are associated to reducing the number of physical prototyping. According to Gidaspow (1994), rarely are reported in terms of detailed economical figures.

Traditionally, two approaches are followed when study multiphase flow phenomena with CFD: Euler–Lagrange and the Euler–Euler. The first, which involves the balance of forces at work upon the particle, requires considerable computational effort. The Euler–Euler approach considers the dispersed phase as a continuous phase and is based on the Navier–Stokes equations applied to each phase (Wen and Yu, 1966; Anderson and Jackson, 1967; Syamlal and O'Brien, 1989; Gidaspow, *et al*., 1992; Taghipour, *et al*., 2005; Duarte, *et al*., 2009; Asegehegn, *et al*., 2011).

An important aspect which influences the accuracy of CFD results for fluidized beds is the methodology used to extract the data. The data extraction methodology and the subsequent results, such as bed properties, bubble characteristics and bed expansion, suffers from great variation between studies reported in the literature (Asegehegn, *et al*., 2011). Also, according to Asegehegn, *et al*., (2011), data extraction can have as much influence as the use of different constitutive relationships. For instance, Hulme, *et al*., (2005), has shown that different volumetric solids fraction at the inlet led to different bubble average parameters. In the literature is also show different ways to define bed expansion ratio (Lofstrand, *et al*., 1995; Geldart, 2004; Taghipour, *et al*., 2005).

Another important parameter that influences the simulation results is the time span used for extracting average quantities. Patil, *et al*., (2005), demonstrated that for different simulation time led to different bubble diameters. The time span depends on parameters, such as bed geometry and superficial velocity, therefore becoming difficult provide a general rule for all operating conditions. On the other hand, greater simulation times yields good results at greater computational expenses.

One of most relevant parameters for fluidized systems is the minimum fluidization velocity (u_{mf}). According to Law and Mujumbar (2006), fluidized bed operate normally at gas velocities to 2-4 times u_{mf}.

In this study we revisit the gas fluidization phenomena for a bed constituted from soybean grains. Three different bed height configurations will be used with two different drag term correlations. The CFD code employed is the MFIX-DEM (Multiphase Flow with Interphase eXchange coupled with Discrete Element Method). The results will be compared with experimental data from Soponronnarit, *et al*., (2001).

2. DESCRIPTION OF THE MODEL

MFIX is an open source CFD code developed at the National Energy Technology Laboratory (NETL) for describing the hydrodynamics, heat transfer and chemical reactions in fluid-solids systems. It has been used for describing bubbling and circulating fluidized beds, spouted beds and gasifiers. MFIX calculations give transient data on the three-dimensional distribution of pressure, velocity, temperature, and species mass fractions.

Figure 1 shows the mesh and boundary conditions for the numerical simulations. The pressure measurement points were located at y = 0.0 m and e y = 1.0 m. The simulations were based on the experiments by Soponronnarit *et al.* (2001) for a soybean fluidized bed, operating at three different initial heights: 0.08 m, 0.115 m e 0.15 m. The mesh was two-dimensional cartesian with 20 x 100 cells. Uniformity in the inlet conditions were used for 13 different velocities. The particle diameter was 0.007 m and its density 1200 kg/m^3.

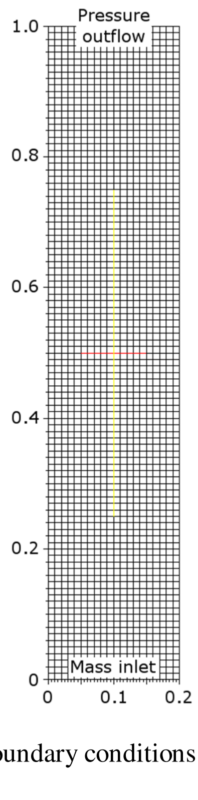

Figure 1. Fluidized bed mesh and boundary conditions to Soponronnarit *et al.* (2001) model

According to Tsuji (2007), particulate system flow can be classified in 3 types: (1) Collisionless; (2) Collision dominated; (3) prolonged contact dominated. The third is subdivided into: fluid absent, fluid present. In this way, fluidized bed flows are classified as 3rd type with presence of fluid.

A second classification by Tsuji (2007) is based on the scales involved in the interaction of fluid and particles, namely: micro, meso and macro. The task of identify boundaries between scales is left to the researcher, but in general, macro models rely on empiricism, whereas micromodels have a sounding theoretical foundation. For this study was employed the E method (micro-particle and meso-fluid) formulated by Tsuji (2007). In this method the particles are tracked (Lagrangian approach) and the fluid is treated in terms of local averaging (Eulerian approach).

2.1 Discrete Element Method (DEM)

DEM, also known as distinct element method, was proposed by Cundall and Strack (1979) for disks and spheres. Based on explicit numerical scheme, the method monitors the contact between particles and their resulting movement. This method is also known as soft-sphere.

In their original work, Cundall and Strack (1979), compared the distinct element method with experiments. The experiments were conducted with optically sensible materials, which allow an accurate determination of contact forces, displacements and rotations, with a great computational cost. Their main conclusion was that the DEM is a valid tool for granular systems. Actually, a great number of open and commercial codes refers to the DEM in describing the dynamics of system with colliding particles, among them fluidized systems. In the DEM, collision and contacts are modeled as a mechanical systems consisting of spring-slider and damper.

Here, material properties such as friction coefficient, spring and damper constant were selected based on the work of Boac *et al.* (2009). Table 1 reports the granular and gas properties employed in the simulations.

The simulation were run for inlet gas velocities ranging from 0.45 m/s to 3.5 m/s with 13 non-uniform increments. For each velocity the simulation time was 3 s.

Table 1. Physical properties, experimental conditions and initial and boundary conditions used in CFD-DEM simulations.

Properties		Literature values	Choice values
Static friction coefficient, μ_s	Particle-particle	0.267; 0.55[(1)]	0.45
	Particle-wall[(4)]	0.30[(1)]	0.30
Particle Restitution Coefficient, e	Particle-particle	0.5; 0.7[(1)]	0.6
	Particle-wall[(4)]	0.6; 0.7[(1)]	0.6
Particle diameter, d_p (x10^{-3} m)			7[(3)]
Particle Length (x10^{-3} m), l		7.0 – 8.2[(1)]	--
Particle Width (x10^{-3} m), w		6.1 – 6.7[(1)]	--
Particle Thickness (x10^{-3} m), t		5.5 – 5.9[(1)]	--
Density of the solid, ρ_s, (kg/m^3)		1130 – 1325.2[(1)]	1200
Bed height of particles, h_{bed} (x10^{-2} m)		8.0; 11.5; 15.0[(2)]	8.0; 11.5; 15.0
Bed height (x10^{-2} m)		100[(2)]	100
Bed width (x10^{-2} m)		20[(2)]	20
Density of the gas (air), ρ_g (kg/m^3)			1.205
Range of inlet air velocity, v_g (m/s)		0.45 – 3.5[(2)]	0.45 – 3.5

[(1)] Boac *et al.* (2009) [(3)] Considered spherical
[(2)] Soponronnarit *et al.* (2001) [(4)] Acrylic

In the beginning of the runs the particles were randomly seeded in the bed interior without touching each other. When the simulation started, under gravity force, the particles settled. This initial bed height corresponded to the heights reported in the Soponronnarit *et al.* (2001) work.

2.2 Governing Equations: Gas phase

In MFIX–DEM, the gas-phase governing equations for mass and momentum conservation are similar to those in traditional gas-phase CFD but with additional coupling terms due to drag from the solids-phase. The solids-phase is modeled using discrete particles. The governing equations, implemented in MFIX (Syamlal, *et al.*, 1993), for the gas-phase continuity and momentum conservation, are:

$$\frac{\partial}{\partial t}\left(\varepsilon_g\, \rho_g\right) + \nabla\left(\varepsilon_g\, \rho_g\, \overrightarrow{v_g}\right) = 0 \tag{1}$$

$$\frac{D}{Dt}\left(\varepsilon_g\, \rho_g\, \overrightarrow{v_g}\right) = \nabla \bullet \overline{\overline{S_g}} + \varepsilon_g\, \rho_g \vec{g} - \sum_{m=1}^{M} I_{gm} \tag{2}$$

where, ε_g is the gas-phase volume fraction, ρ_g is the density of gas-phase, $\overrightarrow{v_g}$ is the volume-averaged gas-phase velocity, I_{gm} is the momentum transfer term between the gas and the mth solid phase, and $\overline{\overline{S_g}}$ is the stress tensor in gas-phase given by:

$$\bar{\bar{S}}_g = -P_g \bar{\bar{I}} + \bar{\bar{\tau}}_g \tag{3}$$

where P_g is the gas-phase pressure. The stress tensor in the viscous regime, $\bar{\bar{\tau}}_g$, is assumed with Newtonian and given by:

$$\bar{\bar{\tau}}_g = 2\mu_g \overline{\overline{D}}_g + \lambda_g tr\left(\overline{\overline{D}}_g\right)\bar{\bar{I}} \tag{4}$$

The tensor $\bar{\bar{I}}$ can be identified like the deformation rate to the gas-phase $\overline{\overline{D}}_g$, given by:

$$\overline{\overline{D_g}} = \frac{1}{2}\left[\nabla\vec{v}_g + \left(\nabla\vec{v}_g\right)^T\right] \tag{5}$$

2.3 Governing Equations: Solid phase

In the DEM approach, the m^{th} solid–phase is represented by N_m spherical particles with each particle having diameter D_m and density ρ_{sm}. Solid phases are differentiated based according to radii and densities. For total of M solid phases, the total number of particles is equal to

$$N = \sum_{m=1}^{N} N_m \tag{6}$$

These N particles are represented in a Lagrangian frame of reference at time t by:

$$X^{(i)}(t), V^{(i)}(t), \omega^{(i)}(t), D^{(i)}, \rho^{(i)} \quad i = 1 \ldots\ldots N \tag{7}$$

where $X^{(i)}(t)$ denotes the i^{th} particle position, $V^{(i)}(t)$ e $\omega^{(i)}(t)$ denote its linear and angular velocities, $D^{(i)}$ denotes its diameter, and $\rho^{(i)}$ represents its density.
The position, the angular and linear velocities of the i^{th} particle evolve according to Newton's laws as:

$$\frac{dX^{(i)}(t)}{dt} = V^{(i)}(t) \tag{8}$$

$$m\frac{dV^{(i)}(t)}{dt} = F_T^{(i)} \tag{9}$$

$$F_T^{(i)} = m^i g + F_d^{(i\in k,m)}(t) + F_c^{(i)}(t) \tag{10}$$

$$I^i \frac{dw^{(i)}(t)}{dt} = T^i \tag{11}$$

where g is the gravity acceleration, $F_{\mathrm{d}}^{(i\in k,m)}$ is the total drag force on i^{th} particle residing in k^{th} cell and belonging to the m^{th} solid-phase, $F_{\mathrm{c}}^{(i)}$ is the net contact force acting as a result of contact with other particles, T^i is the sum of all torques acting on the ith particle, and $F_{\mathrm{T}}^{(i)}$ is the net sum of all forces acting on the i^{th} particle.

A advantage at DEM is the manner like it is solve the equations to the solid phase, taking to explicit treatment of particle-particle collisions. To solid-gas flows at MFIX-DEM is employed the Cundall and Strack (1979) model, also know like soft-sphere model.

To the drag force calculation, is used the follow model:

$$F_{\mathrm{d}}^{(i\in k,m)} = -\nabla \mathrm{P_g}(\mathrm{x_k})\mathcal{V}_\mathrm{m} + \frac{\beta_\mathrm{m}^{(\mathrm{k})}\mathcal{V}_\mathrm{m}}{\varepsilon_\mathrm{sm}}\left(\mathrm{v_g}(\mathrm{x_k}) - \mathrm{v_{sm}}(\mathrm{x_k})\right) \tag{12}$$

where $P_\mathrm{g}(\mathrm{x}_k)$ and $\mathrm{v_g}(\mathrm{x}_k)$ are the gas–phase mean pressure P_g and velocity $\mathrm{v_g}$ fields at the k^{th} particle location, $\mathcal{V}_m$ is the particle volume, and $\beta_m^{(k)}$ is the local gas-solid momentum transfer coefficient for k^{th} cell.

The $\beta_m^{(k)}$ represent the drag coefficient with different models developed and can be write by:

$$\beta_\mathrm{m}^{(\forall i\in k)} = \beta_\mathrm{m}^{(\mathrm{k})} = \left(\rho_\mathrm{m}, \mathrm{D_m}, \left|\mathrm{v_{sm}}(\mathrm{x_k}) - \mathrm{v_g}(\mathrm{x_k})\right|, \rho_\mathrm{g}, \mu_g\right) \tag{13}$$

where x_k is the center of the k^{th} cell, $\mathrm{v_g}\left(X^{(i)}\right)$ is the gas-phase mean velocity in the $X^{(i)}$ position, where a cell-centered value of $\mathrm{v_g}$ is used. Similarly, $\mathrm{v_{sm}}$ is a local cell average velocity of the m^{th} solid-phase.

If considered a approximation of the constant drag force for all particles in a particular cell, the gas-solid momentum transfer $I_{\mathrm{gm}}^{(k)}$ is estimated to the k^{th} cell by

$$I_{\mathrm{gm}}^{(k)} = \varepsilon_\mathrm{sm}\nabla \mathrm{P_g}(\mathrm{x_k}) + \beta_\mathrm{m}^{(\mathrm{k})}\left(\mathrm{v_g}(\mathrm{x_k}) - \mathrm{v_{sm}}(\mathrm{x_k})\right) \tag{14}$$

3. RESULTS

The results for pressure drop were obtained from the post processing command line post_mfix utility available in the MFIX code. Figures 2, 3 and 4, were generated with Paraview software (2015), and depict the volumetric fields and particle positions for beds with different initial height.

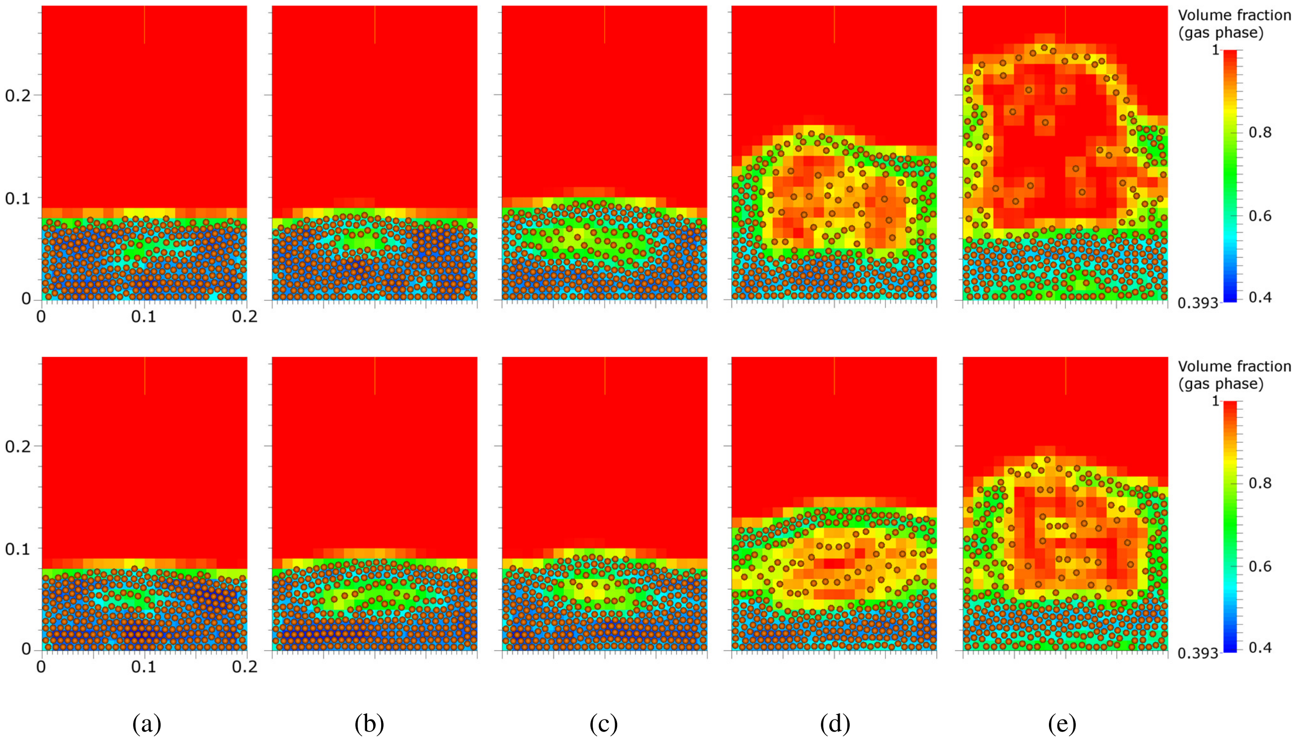

Figure 2. First bubble formation after velocity change with h_{bed} = 0.080 m: Gidaspow (above) *vs.* Syamlal (bellow). Gas velocity: (a) 2.1 m/s, (b) 2.2 m/s, (c) 2.3 m/s, (d) 2.8 m/s and (e) 3.5 m/s

Concerning to the bed hydrodynamics, it can be seen that Gidaspow drag, corresponds to a slightly greater bubble formation in the central region. Supplementally, the influence of turbulence is more highlighted for this drag model. This can be noticed by the horizontal lining up in the regions where the gas voidage is in the 0.6-0.9 range. These phenomena are better depicted when comparing the figures for velocities near the minimum fluidization (a, b and c, Fig. 2 and Fig. 3).

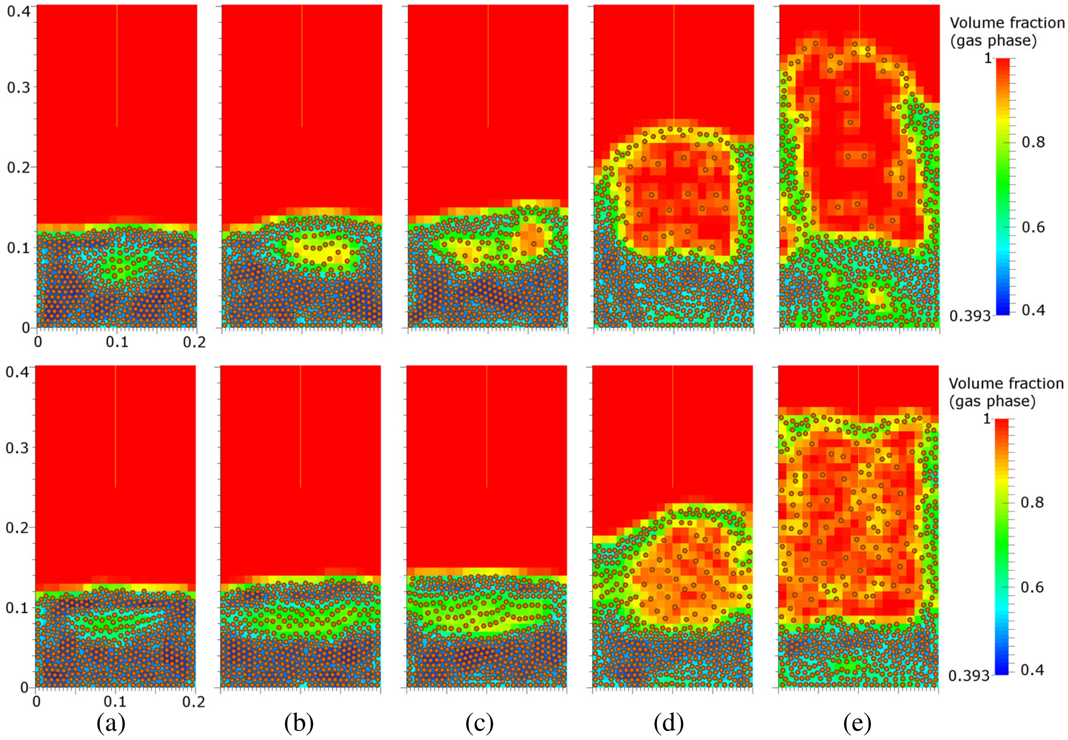

Figure 3. First bubble formation after velocity change with h_{bed} = 0.115 m: Gidaspow (above) *vs.* Syamlal (bellow). Gas velocity: (a) 2.1 m/s, (b) 2.2 m/s, (c) 2.3 m/s, (d) 2.8 m/s and (e) 3.5 m/s

From analysis of Fig. 4d e Fig. 4e is noticed a greater dense bed height when the Gidaspow drag is employed.

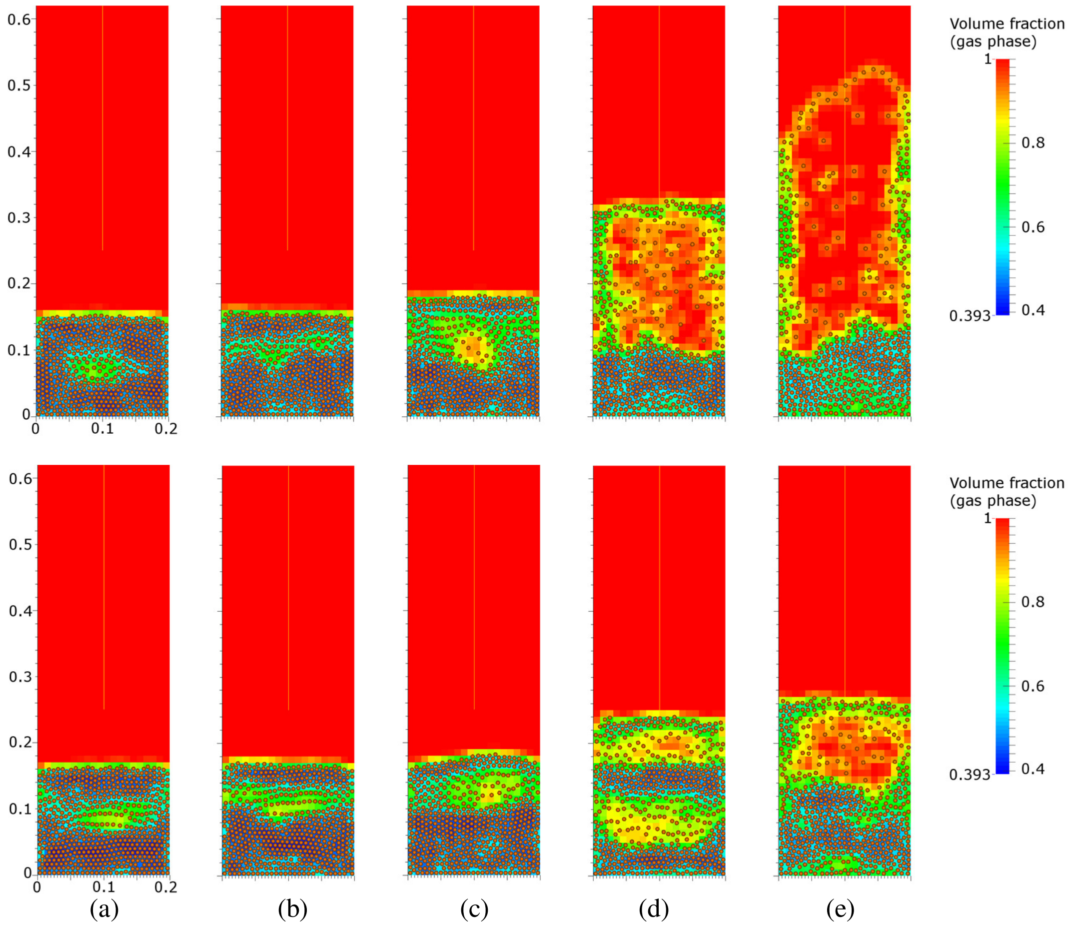

Figure 4. First bubble formation after velocity change with h_{bed} = 0.150 m: Gidaspow (above) *vs.* Syamlal (bellow). Gas velocity: (a) 2.1 m/s, (b) 2.2 m/s, (c) 2.3 m/s, (d) 2.8 m/s and (e) 3.5 m/s

Figure 5 and Fig. 6 show the bed pressure drop versus air superficial velocity. Gray dotted lines corresponds to experimental data from Soponronnarit *et al*. (2001). Continuous lines corresponds to time averaged values extracted from CFD-DEM simulations for each air superficial velocity. It was verified that an increase in bed height correlates with a increase in pressure drop.

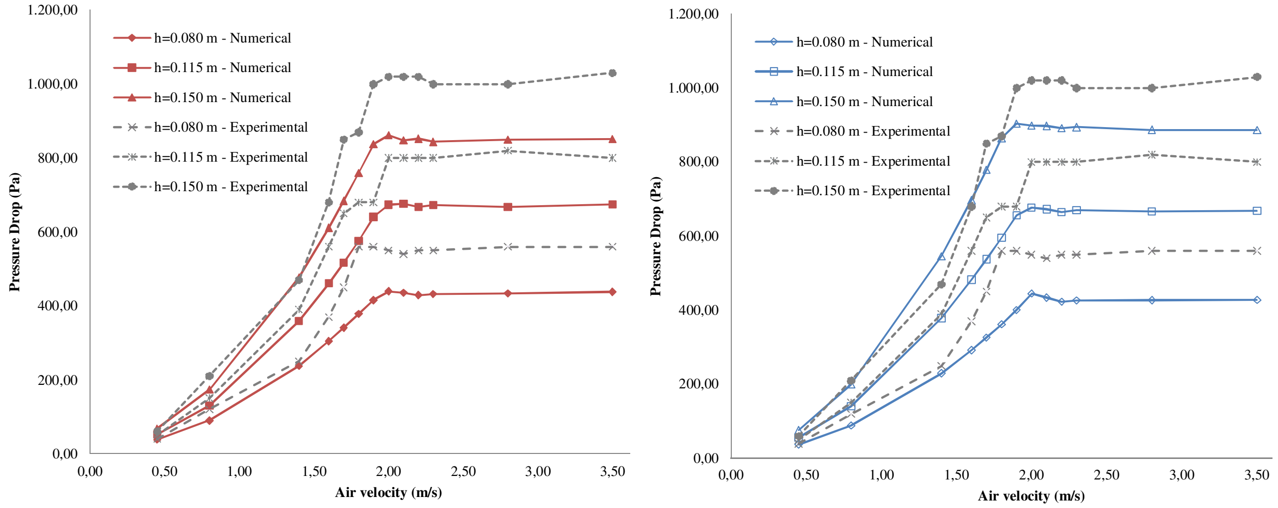

(a) (b)

Figure 5. Pressure drop *versus* inlet air velocity diagram: (a) Gidaspow and (b) Syamlal

Besides the noticeable influence of the drag models used in the CFD-DEM simulations on the particles dynamics (Fig. 2, Fig. 3 and Fig. 4), it is verified that the pressure drop is not significantly affected (Fig. 6). For the bed with 0.150 m height analyzed with Syamlal drag, the minimum fluidization velocity was 1.9 m/s. For all the other cases, the simulation results predicted a minimum fluidization velocity of 2 m/s.

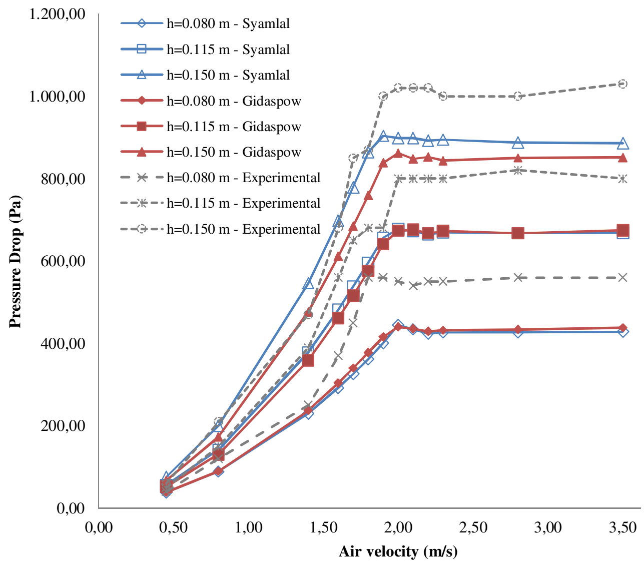

Figure 6. Pressure drop *versus* inlet air velocity diagram: Gidaspow *versus* Syamlal

Figure 6 shows that only for the bed with 0.150 m height there is a deviation in the curves that shows the pressure drop. Regarding the greater differences for pressure drop between numerical and experimental values for greater gas velocities, this can attributed to a stronger interaction between particles, that can lead a more fluctuating pressure value.

4. CONCLUSIONS

The CFD-DEM coupled method yields good results for predicting the minimum fluidization velocity for the studied cases, where numerical values are slightly higher compared to the Soponronnarit *et al*. (2001) experimental values, 2.0 m/s versus 1.9 m/s, respectively.

The differences for pressure loss between numerical and experimental values are more relevant; however, the curve trends are analogous. A identified shortcoming resides in the several parameters of DEM were extracted from literature, not being granted to represent the solids particles.

For future work, different drag models as well the assembly of a new experimental rig are being planned.

5. ACKNOWLEDGEMENTS

The authors would like to thank CAPES and Araucária Foundation for financial support and the National Supercomputing Center (CESUP), of the Federal University of Rio Grande do Sul (UFRGS) for the availability of resources and technology for the development of this research.

6. REFERENCES

Anderson, T.B., Jackson, R., 1967. A Fluid Mechanical Description of Fluidized Beds Equations of Motion, *Industrial e Engineering Chemistry Fundamentals*, Vol. 6 (4), p. 527-539

Asegehegn, T. W., Krautz, H. J. Schreiber, M., 2011. Numerical Study of a Gás-Sólid Fluidized Beds Hydrodynamics: Influence of Immersed Horizontal Tubes and Data Analysis. *International Journal of Chemical Reactor Engineering*, Vol. 9 (1), p. 1-39.

Boac, J.M., Casada, M.E., Maghirang, R.G., Harner, J.P, 2009. Material and Interaction Properties of Selected Grains and Oilseeds for Modeling Discrete Particles. *ASABE Annual International Meeting*, Paper Number 09-7166.

Duarte, C.R., Olazar, M., Murata, V.V., Barrozo, M.A.S. 2009. Numerical simulation and experimental study of fluid–particle flows in a spouted bed. *Powder Technology*, Vol. 188, p. 195-205.

Geldart, D., 2004. Expansion of Gas Fluidized Beds. *Industrial e Engineering Chemistry Research*, Vol. 43 (18), p. 5802-5809.

Gidaspow, D., 1994. *Multiphase Flow and Fluidization: Continuum and Kinetic Theory Descriptions.* Academic Press, Boston.

Gidaspow, D., Bezburuah, R., Ding, J., 1992. Hydrodynamics of circulating fluidized beds, kinetic theory approach in fluidization, *Proceedings of the 7th Engineering Foundation Conference on Fluidization*, p. 75-82.

Hulme, I., Clavelle, E., Van Der Lee, L., Kantzas, A., 2005. CFD Modeling and Validation of Bubble Properties for a Bubbling Fluidized Bed. *Industrial e Engineering Chemistry Research*, Vol. 44 (12), p. 4254-4266.

Kunii, D., Levenspiel, O. 1991. *Fluidization Engineering*. John Wiley & Sons: New York, p. 491.

Law, C. L., Mujumdar, A. S., 2006. *Fluid Bed Dryers. In Handbook of Industrial Drying*. Taylor & Francis. Cap. 8, p 174-199.

Lofstrand, H., Almsted, A. E.,Anderson, S., 1995. Dimensionless Expansion Model for Bubbling Fluidized Beds with and without Internal Heat Exchanger Tubes. *Chemical Engineering Science*, Vol. 50 (2), p. 245-253.

Soponronnarit, S., Swasdisevi, T., Wetchacama, S., Wutiwiwatchai, W., 2001. Fluidised bed drying of soybeans. *Journal of Stored Products Research*, Vol. 37, p. 133-151.

Syamlal, M., O'Brien, T.J., 1989. Computer simulation of bubbles in a fluidized bed. *AIChE Symp. Ser.*, Vol. 85, p. 22–31.

Tsuji, Y., Kawaguchi, T. and Tanaka, T., 1993. Discrete particle simulation of two-dimensional fluidized bed. *Powder Technology*, Vol. 77, p. 79-87.

Taghipour, F., Ellis, N., Wong, C., 2005, Experimental and computational study of gas–solid fluidized bed hydrodynamics, *Chem. Eng. Sci.*, Vol. 60, p. 6857-6867.

Wen, C.Y., Yu, Y.H., 1966. Mechanics of fluidization, *Chem. Eng. Prog. Symp. Ser.*, Vol. 62, p. 100–111.

7. RESPONSIBILITY NOTICE

The authors are the only responsible for the printed material included in this paper.